

Silencing of *ERRα* gene represses cell proliferation and induces apoptosis in human skin fibroblasts

NAOKI NANASHIMA^{1,2}, TOSHIO NORIKURA¹, MANABU NAKANO², CHIE HATA³ and KAYO HORIE²

¹Department of Nutrition, Faculty of Health Science, Aomori University of Health and Welfare, Aomori 030-8505, Japan;

²Department of Bioscience and Laboratory Medicine, Hirosaki University Graduate School of Health Sciences, Hirosaki, Aomori 036-8564, Japan; ³Department of Biomedical Data Intelligence, Graduate School of Medicine,

Kyoto University, Kyoto 606-8397, Japan

Received January 25, 2024; Accepted August 9, 2024

DOI: 10.3892/mmr.2024.13370

Abstract. Estrogen-related receptor (ERR) is an orphan nuclear receptor structurally akin to the estrogen receptor. ERR is expressed in tissues with active energy metabolism and regulates intracellular metabolic functions. Additionally, ERRs are known to be strongly expressed in the epidermis of skin tissue, but their functions are unknown. The present study investigated the function of *ERRα* in human skin fibroblasts. *ERRα* expressed in human dermal fibroblast TIG113 was knocked down using small interfering (si)RNA and gene expression was comprehensively analyzed using microarrays 48 h later. Pathway analysis was performed using Wikipathways on genes exhibiting expression changes of ≥ 1.5 -fold. Expression of cell cycle-related and apoptosis-related genes was compared using reverse transcription-quantitative PCR. After treating TIG113 cells with si*ERRα* for 72 h, cell proliferation was assessed using the Cell Counting Kit-8 or a scratch wound healing assay and apoptotic cells were measured using the Poly Caspase Assay Kit. Cell cycle analysis was performed using flow cytometry. The expression of the *ERRα* gene was suppressed by siRNA. The expression of genes associated with cell cycle-related pathways were decreased while that of those associated with apoptosis-related pathways increased. Furthermore, the expression of cell cycle-related genes such as cell division cycle 25C, cyclin E and cyclin B1 was decreased and the expression of apoptosis-related genes such as caspase3 and Fas cell surface death receptor was increased.

Cell proliferation was suppressed and the number of apoptotic cells increased ~ 2 -fold in *ERRα*-knockdown TIG113 cells. Cell cycle analysis revealed that the number of cells in the Sub-G₁ phase increased and that in the S and G₂/M phases decreased. The present study suggested that *ERRα* is an essential for the survival of human skin fibroblasts.

Introduction

Estrogen-related receptor (ERR) has a similar structure to that of estrogen receptor and is an orphan nuclear receptor whose endogenous ligand is unknown (1). ERR has a high homology with the DNA-binding domain of the estrogen receptor and binds to the estrogen-responsive element on the promoter. However, it has low homology with the ligand-binding domain and estrogen does not act as a ligand for ERR (1,2).

ERRα, *ERRβ* and *ERRγ* are the three subtypes of ERR. *ERRα* and *ERRγ* are expressed in tissues with active energy metabolism, such as the heart, kidneys, skeletal muscle and adipose tissues (3,4). In addition, it has been reported that *ERRα* and *ERRγ* regulate intracellular metabolic functions, such as oxidative phosphorylation in mitochondria (5-7). It has further been reported that *ERRβ* is expressed in the placenta and villous tissue and involved in placenta formation (8).

Estrogen regulates a variety of physiological and disease processes, including reproduction, bone remodeling and breast cancer, among others. It has been revealed that ERR shares target genes and regulatory proteins with estrogen receptor (9). Furthermore, ERR actively influences estrogen responses and it has been suggested that pharmacologically modulating ERR activity may be useful for the prevention and treatment of various symptoms related to women's health (9).

The skin is an estrogen-sensitive organ and skin fibroblasts produce extracellular matrix components, such as collagen, hyaluronic acid and elastin (10-12). These components are also related to skin antiaging and wrinkles and sagging of the skin are likely to occur in menopausal women owing to the decreased secretion of estrogen (10). Furthermore, skin fibroblasts express estrogen receptors α and β and are susceptible to estrogen (13). As ERR interacts with estrogen signaling (14) and is expressed in the skin, it may also play an important role in skin antiaging.

Correspondence to: Professor Naoki Nanashima, Department of Nutrition, Faculty of Health Science, Aomori University of Health and Welfare, 58-1 Mase, Hamadate, Aomori 030-8505, Japan
E-mail: n_nanashima@ms.auhw.ac.jp

Abbreviations: CASP3, caspase 3; CDC25C, cell division cycle 25C; ERR, Estrogen-related receptor; FAS, Fas cell surface death receptor; PGC-1 α , peroxisome proliferator-activated receptor gamma, coactivator 1 α

Key words: apoptosis, cell proliferation, estrogen-related receptor α , skin fibroblast

In normal human skin, *ERRα* and *ERRβ* are expressed in epidermal keratinocytes (15,16) and *ERRγ* is expressed in keratinocytes and fibroblasts (17). However, their functions remain unknown.

The present study analyzed the function of *ERRα* in human skin fibroblasts by silencing its gene expression. It performed microarray and pathway analyses and reverse transcription quantitative (RT-q) PCR. Cell proliferation and apoptosis-positive cells were examined and the cell cycle was analyzed using flow cytometry. The present study is the first to report the function of *ERRα* in human skin fibroblasts, to the best of the authors' knowledge.

Materials and methods

Cell culture. Human normal adult skin fibroblasts (TIG113; JCRB0539) and human neonatal foreskin fibroblasts (NFF; KF-4009, passage 2, <https://www.kurabo.co.jp/bio/cell-tissue/skin/03/>) were obtained from the Health Science Research Resources Bank (Japan) and KURABO, respectively. The cells were maintained in Dulbecco's modified Eagle's medium (DMEM; FUJIFILM Wako Pure Chemical Corporation) with 10% fetal bovine serum (Sigma-Aldrich; Merck KGaA), 100 units/ml penicillin and 100 μ g/ml streptomycin (FUJIFILM Wako Pure Chemical Corporation). All culture experiments were conducted at 37°C in a humidified incubator supplemented with 5% CO₂.

Small interfering (si)RNA transfection. The expression of the human *ERRα* gene was silenced using transient transfection of *ERRα* siRNA (si*ERRα*; cat. no. sc-44706; Santa Cruz Biotechnology, Inc.), which was performed using DharmaFECT 1 transfection reagent (Horizon Discovery Ltd.), according to the manufacturer's instructions. TIG113 cells were incubated with 50 nM siRNA at 37°C for 24–72 h before use in subsequent assays. As a negative control, TIG113 cells were transfected with Silencer Negative Control #1 siRNA (siNC; cat. no. 4390843; Thermo Fisher Scientific, Inc.).

Microarray analysis and Wikipathways. TIG113 cells were seeded in a 100-mm cell culture dish, cultured until 80% confluence as described in the *Cell culture* section and then transfected with si*ERRα* or siNC. After 48 h, total RNA was extracted using the RNeasy Mini kit (Qiagen GmbH), according to the manufacturer's instructions.

The RNA (1 μ g) was used to produce biotin-labeled complementary RNA (cRNA). The labeled and fragmented cRNA was subsequently hybridized to the SurePrint G3 Human Gene Expression microarray (8x60 K ver. 3; Agilent Technologies Inc.). Labeling, hybridization, image scanning and data analysis were performed at Macrogen Japan and the Research Institute of Bio-System Informatics (Iwate, Japan). The TIG113 microarray datasets are available at <http://www.ncbi.nlm.nih.gov/geo> under accession code GSE245234 (<https://www.ncbi.nlm.nih.gov/geo/query/acc.cgi?acc=GSE245234>). The ratio of gene expression change in cells treated with si*ERRα* to that in cells treated with siNC was expressed as fold change. Genes with 1.5-fold or greater upregulation or downregulation (n=3) following siRNA transfection in TIG113 cells were subjected to biological pathway enrichment analyses using Wikipathways (version number 20201210; <https://www.wikipathways.org/>).

Reverse transcription-quantitative (RT-q) PCR. TIG113 cells were seeded in 6-well plates and cultured as described in the *Cell culture* section until they reached 80% confluence and were then transfected with si*ERRα* or siNC. After incubating at 37°C for 48 h, cells were washed twice with PBS. Total RNA was extracted from the TIG113 cells using the RNeasy mini kit (Qiagen KK) according to the manufacturer's instructions. cDNA was reverse-transcribed from total RNA using the PrimeScript RT Master Mix (Takara Bio, Inc.) according to the manufacturer's instructions. Levels of each mRNAs were quantified by qPCR using TB Green Premix Ex Taq II (Tli RNaseH Plus; Takara Bio, Inc.). The thermocycling conditions were as follows: 30 sec at 95°C, followed by 40 cycles of 5 sec at 95°C and 30 sec at 60°C. Transcription levels were normalized to those of *GAPDH* cDNA. The primer sequences were as follows (5'-3'): *ERRα*, forward GGCCCTTGCCAA TTCAGA and reverse GGCCTCGTGCAGAGCTTCT (18); *ERRβ*, forward GTCTCATACCTACTGGTGGC and reverse AGGTCACAGAGAGTGGTCAG (19); *ERRγ*, forward CAG ACGCCAGTGGGAGCTA and reverse TGGCGAGTCAAG TCCGTTCT (19); *CDKN1C*, forward GCGGCGATCAAG AAGCTGTC and reverse CCGGTTGCTGCTACATGA AC (20); peroxisome proliferator-activated receptor gamma, coactivator 1 alpha (*PGC-1α*), forward AGCCTCTTTGCC CAGATCTT and reverse GGCAATCCGTTTCATCC AC (21); caspase 3 (*CASP3*), forward GCGGTTGTAGAA GAGTTTCGTG and reverse CTCACGGCCTGGGATTC AA (22); Fas cell surface death receptor (*FAS*), forward CAA TTCTGCCATAAGCCCTGTC and reverse GTCCTTCAT CACACAATCTACATCTT (23); cell division cycle 25C (*CDC25C*), forward GCAGAAGTGGCCTATATCGCT and reverse TTCCACCTGCTTCAGTCTTGG (24); cyclin E2 (*CCNE2*), forward TCAAGACGAAGTAGCCGTTTAC and reverse TGACATCCTGGGTAGTTTTCTC (25); cyclin B1 (*CCNB1*), forward AATAAGGCGAAGATCAACATG GC and reverse TTTGTTACCAATGTCCCAAGAG (26); and *GAPDH* (NM_001256799.3), forward TGAGAACGG GAAGCTTGTC and reverse TCTCCATGGTGGTGAAGA CG. The *GAPDH* primers were designed using the Primer 3 Plus interface (<https://www.bioinformatics.nl/cgi-bin/primer3plus/primer3plus.cgi>). PCR specificity was assessed using melting curve analysis. All samples were analyzed in duplicate and relative gene expression was calculated using the 2^{- $\Delta\Delta$ C_q} method (27). Three independent experiments were performed.

Western blotting. TIG113 cells were seeded in 30-mm plates and cultured as described in the *Cell culture* section until they reached 80% confluence and then transfected with si*ERRα* or siNC. After incubating at 37°C for 72 h, cells were washed twice with PBS. TIG113 cell lysates were prepared with RIPA lysis buffer (Santa Cruz Biotechnology, Inc.). The protein concentrations were determined using a Takara BCA Protein Assay kit (Takara Bio, Inc.). Total protein (20 μ g/lane) was separated by SDS-polyacrylamide gel electrophoresis on 12% (w/v) polyacrylamide gels and was electroblotted onto Hybond nitrocellulose membranes (Cytiva). Subsequently, blocking was performed with 3% non-fat milk powder at room temperature for 2 h. Blots were probed with anti-*ERRα* antibody (cat. no. 13826; Cell Signaling Technology, Inc.; 1:300) or anti- β -actin antibody (cat. no. 81115-1-RR; Proteintech

Group, Inc.; 1:1,000) at 4°C overnight, followed by incubation with horseradish peroxidase-conjugated anti-rabbit IgG (cat. no. ab6721; Abcam; 1:2,000) at room temperature for 1.5 h. The signal was detected using ImmunoStar Zeta (FUJIFILM Wako Pure Chemical Corporation), according to the manufacturer's protocol. Luminescent images were analyzed using a LumiCube (Liponics).

Cell proliferation assay. A total of 4,000 TIG113 cells were seeded in a 96-well plate, cultured as described in the *Cell culture* section for 24 h and then transfected with siRNA. TIG113 cell proliferation was analyzed with a Cell Counting Kit-8 (CCK-8; Dojindo Laboratories, Inc.) following the manufacturer's protocol. Briefly, the CCK-8 reagent was added to the cells for 1.5 h at 37°C. Absorbance was measured on a Benchmark microplate reader (Bio-Rad Laboratories, Inc.) at a wavelength of 450 nm. The number of cells treated with siNC for 0 h was defined as 100% and the increase rate at each time point was expressed as a percentage.

Scratch wound healing assay. TIG113 cells were seeded in triplicate 6-well plates and cultured as described in the *Cell culture* section until they reached 80% confluence and then transfected with siERR α or siNC in DMEM containing 10% fetal bovine serum. After 24 h, the surface of the dishes was scratched linearly with a 200- μ l pipette tip and the cells were incubated in serum-free DMEM for 48 h at 37°C. Images were captured using a phase-contrast and an inverted microscope (CK40; Olympus Corporation; magnification, x40) equipped with an Anyty digital microscope camera (3R-DKMCO4; 3R solution). The wound area for each treatment was calculated by averaging three individual measurements at 0 and 48 h using ImageJ software (ver.1.53; National Institutes of Health). Cell migration was expressed as the percentage of the scratch area filled by migrating cells 48 h post-scratch: migration (%)=(scratch area at 0 h-scratch area at 48 h/scratch area at 0 h) x100.

Apoptosis detection. A total of 4,000 TIG113 cells were seeded in a 96-well plate, cultured as described in the *Cell culture* section for 24 h and then transfected with siERR α or siNC. After 72 h, apoptosis was detected using the Poly Caspase Assay Kit Green FLICA (ImmunoChemistry Technologies, LLC). Relative fluorescent units were measured using a Tecan Infinite 200 Pro Microplate reader (excitation, 530 nm; emission, 590 nm; Tecan Group, Ltd.).

Cell cycle analysis. Cell cycle analysis was performed as in our previous study (28). Briefly, TIG113 cells were seeded in a 100-mm cell culture dish and cultured as described in the *Cell culture* section until they reached 80% confluence. Cells were transfected with siERR α or siNC and cultured for 72 h prior to DNA staining. Cells were washed in PBS, resuspended in propidium iodide (PI)/RNase Staining Buffer (BD Biosciences) and incubated for 15 min at 25°C. PI fluorescence (FL3) was measured using an FC500 flow cytometer (Beckman Coulter, Inc.). Data were analyzed using the MultiCycle AV software (Phoenix Flow Systems).

Type I collagen and hyaluronan quantification in the medium. TIG113 cells were seeded in a 30-mm cell culture dish, cultured as described in the *Cell culture* section until they reached 80%

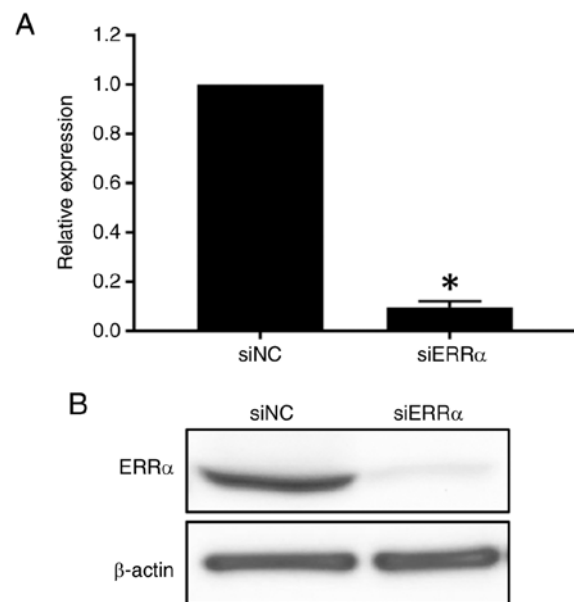


Figure 1. Silencing of ERR α in TIG113 cells. TIG113 cells were transfected with siERR α or a siNC and cultured for 48-72 h. (A) The level of ERR α mRNA expression 48 h after siRNA transfection was evaluated using reverse transcription-quantitative PCR. (B) ERR α protein after 72 h after siERR α transfection was evaluated using western blotting. The data represent the mean \pm standard deviation of at least three independent experiments. * $P < 0.05$ vs. siNC. ERR α , estrogen-related receptor α ; si, small interfering; NC, negative control.

confluence and were then transfected with siERR α or siNC. After 72 h, the supernatant was collected and filtered through a sterile filter (0.2 μ m). Type I collagen and hyaluronan secreted into the medium were quantified using a human collagen type I enzyme-linked immunosorbent assay (ELISA) kit (cat. no. EC1-E105; ACEL, Inc.) and Hyaluronan Quantification Kit (cat. no. HA-KIT; Iwai Chemicals Company, Co., Ltd.), respectively, following the manufacturer's instructions.

Statistical analysis. The results are expressed as mean \pm standard deviation. Statistically significant differences were determined using Welch's t-test or Kruskal-Wallis analysis with the Steel post-hoc test between two groups and multiple groups, respectively, using Bell Curve for Excel ver. 4.04 (Social Survey Research Information Co., Ltd.). Wikipathways that were significant were determined by Fisher's Exact Test. Furthermore, p.adjust was calculated by performing multiple testing corrections using the Benjamini-Hochberg method. Values with p.adjust < 0.05 were considered statistically significant. $P < 0.05$ was considered to indicate a statistically significant difference.

Results

Expression of ERRs and ERR α silencing. To investigate the function of ERR α in human skin fibroblasts, ERR α expression in TIG113 cells was suppressed using siRNA targeting ERR α . The ERR α siRNA (siERR α) significantly decreased ERR α expression at the mRNA level compared with a nontargeting control (siNC; $P < 0.05$; Fig. 1A). Furthermore, western blot analysis revealed that the ERR α expression was reduced in

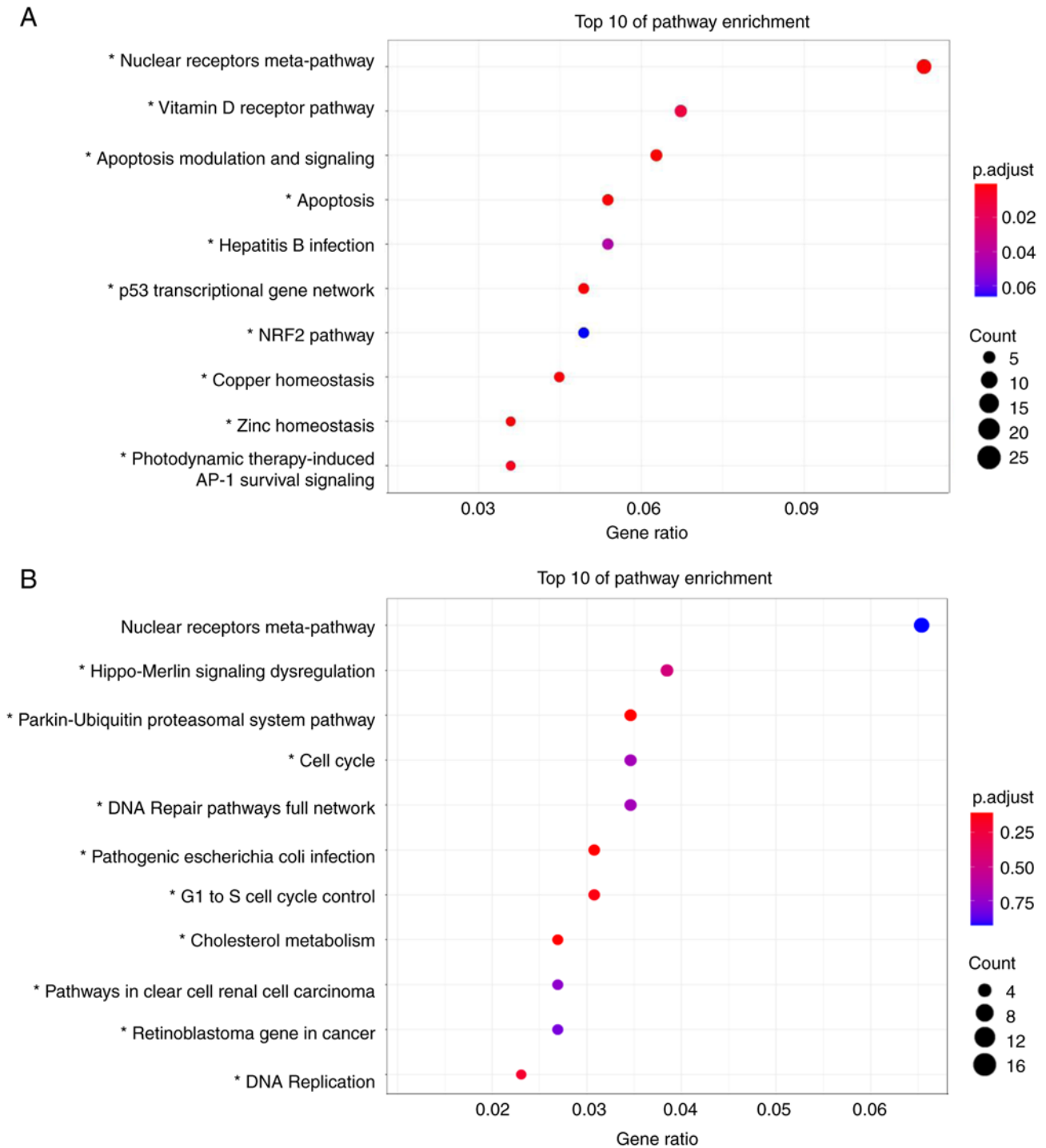


Figure 2. Wikipathways analysis in *ERRα*-silenced TIG113 cells. (A) Upregulated top 10 enrichment pathways were analyzed using Wikipathways for 48 h si*ERRα* transfection. (B) Downregulated top 10 enrichment pathways were analyzed using Wikipathways for 48 h si*ERRα* transfection. * $P < 0.05$. *ERRα*, estrogen-related receptor α ; si, small interfering.

si*ERRα*-treated TIG113 cells (Fig. 1B). Moreover, microarray analysis revealed that the high expression of *ERRα* compared with that of estrogen receptors α and β suggested the importance of *ERRα* in skin fibroblasts (Table S1). In addition, when the expression of *ERRα*, *ERRβ* and *ERRγ* in TIG113 cells was analyzed using RT-qPCR, the relative expression level of *ERRβ* was only 1.3% that of *ERRα*, and *ERRγ* was not notably expressed ($P < 0.05$; Fig. S1A). The same experiments using human NFFs yielded similar results ($P < 0.05$; Fig. S1B).

Pathways enrichment analysis. Microarray analysis found 580 upregulated and 738 downregulated genes (Table SII) that had a fold change of 1.5-fold upon *ERRα* knockdown ($n=3$). Using the genes whose relative expression changed by 1.5-fold or more, biological pathway analyses in TIG113 cells were performed using Wikipathways. The top 10 upregulated or downregulated pathways detected using Wikipathways are shown in Fig. 2A and B, respectively. The ‘Nuclear Receptors Meta-Pathway’ ranked the highest in upregulated

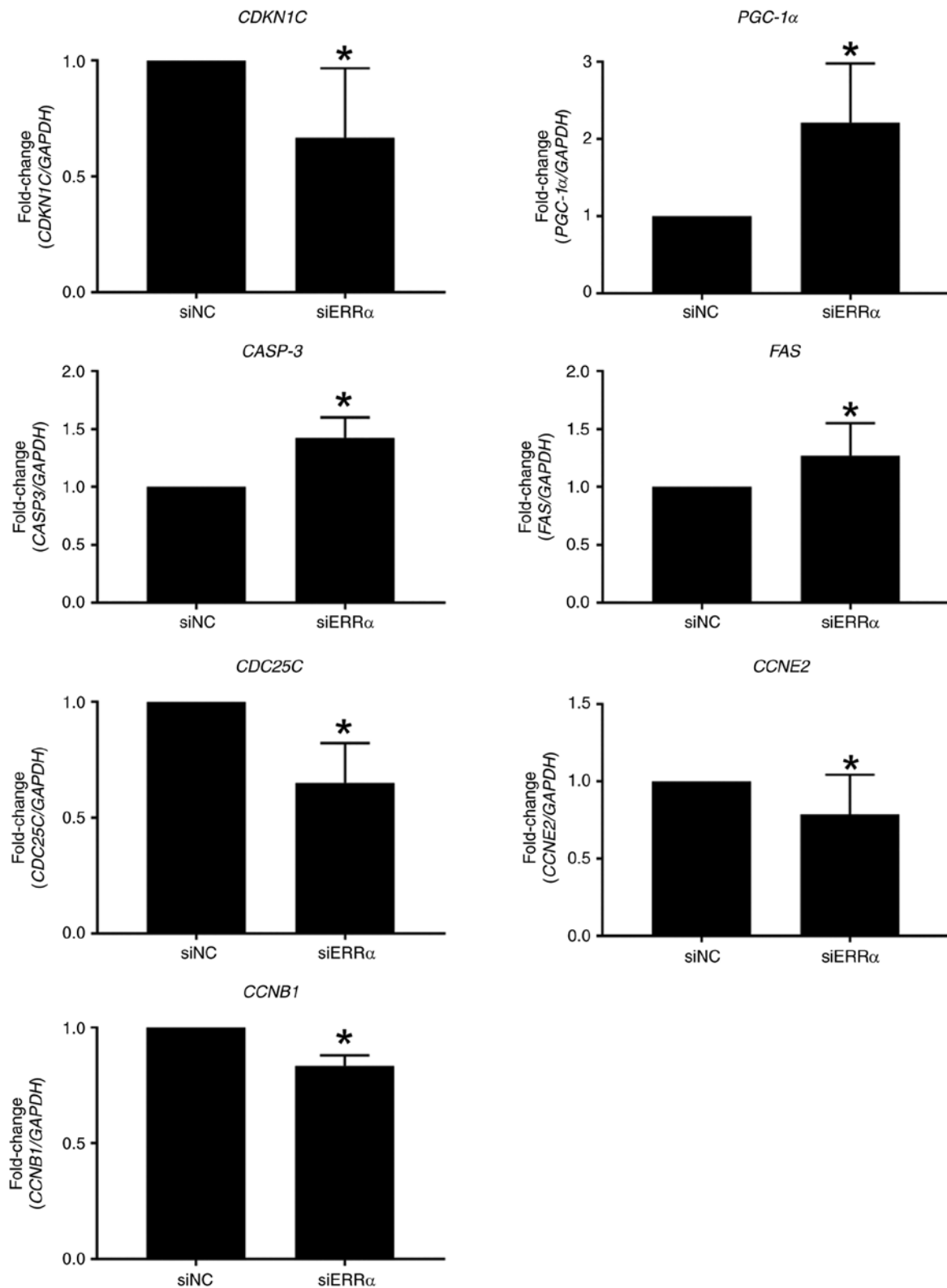


Figure 3. Validation of gene expression in TIG113 cells. TIG113 cells were transfected with siERRα or siNC and cultured for 48 h. The mRNA levels of each gene were quantified using reverse transcription-quantitative PCR. Relative expression was normalized to that of *GAPDH*. Data represent the mean ± standard deviation of three independent experiments. *P<0.05 vs. siNC. *ERRα*, estrogen-related receptor α; si, small interfering; NC, negative control; *CDKN1C*, cyclin-dependent kinase inhibitor 1C; *PGC-1α*, peroxisome proliferator-activated receptor gamma, coactivator 1 α; *CASP3*, caspase 3; *FAS*, Fas cell surface death receptor; *CDC25C*, cell division cycle 25C; *CCNE2*, cyclin E2; *CCNB1*, cyclin B1.

and downregulated pathways, but no significant difference was observed in downregulated pathways. The upregulated pathways were mainly apoptosis-related pathways, such as

'Apoptosis Modulation and Signaling' and 'p53 transcriptional gene network' (Fig. 2A). Furthermore, the downregulated pathways were related to cell cycles such as 'Cell Cycle',

Table I. Fold change of selected gene expression by *ERRα* silencing.

A, Nuclear receptors meta-pathway (upregulation)		
Gene symbol	Gene name	Fold change
<i>TGFB2</i>	Transforming growth factor, β 2	3.65±0.45
<i>SLC2A14</i>	Solute carrier family 2 (facilitated glucose transporter), member 14	3.05±0.31
<i>SLC2A3</i>	Solute carrier family 2 (facilitated glucose transporter), member 3	2.53±0.22
<i>ABCC3</i>	ATP-binding cassette, sub-family C (CFTR/MRP), member 3	2.37±0.30
<i>RGS2</i>	Regulator of G-protein signaling 2	2.77±0.58
<i>CDKN1C</i>	Cyclin-dependent kinase inhibitor 1C (p57, Kip2)	2.21±0.19
<i>PGC-1α</i>	Peroxisome proliferator-activated receptor gamma, coactivator 1 alpha	2.39±0.22
<i>CYP3A5</i>	Cytochrome P450, family 3, subfamily A, polypeptide 5	2.30±0.22
<i>ESR1</i>	Estrogen receptor 1	2.05±0.19
<i>EPHA2</i>	EPH receptor A2	2.10±0.20
<i>CYP3A7</i>	Cytochrome P450, family 3, subfamily A, polypeptide 7	2.41±0.41
<i>SLC7A11</i>	Solute carrier family 7 (anionic amino acid transporter light chain, xc-system), member 11	1.88±0.16
<i>SLC6A6</i>	Solute carrier family 6 (neurotransmitter transporter), member 6	1.94±0.07
<i>CYP1B1</i>	Cytochrome P450, family 1, subfamily B, polypeptide 1	1.73±0.09
<i>SPRY1</i>	Sprouty homolog 1, antagonist of FGF signaling (<i>Drosophila</i>)	1.86±0.40
<i>PK4</i>	Pyruvate dehydrogenase kinase, isozyme 4	2.01±0.34
<i>GCLC</i>	Glutamate-cysteine ligase, catalytic subunit	1.71±0.06
<i>JUNB</i>	Jun B proto-oncogene	1.92±0.27
<i>HBEGF</i>	Heparin-binding EGF-like growth factor	1.61±0.07
<i>SLC7A5</i>	Solute carrier family 7 (amino acid transporter light chain, l system), member 5	1.75±0.06
<i>SLC39A8</i>	Solute carrier family 39 (zinc transporter), member 8	1.76±0.12
<i>PPARA</i>	Peroxisome proliferator-activated receptor alpha	1.71±0.12
<i>LRRC8A</i>	leucine rich repeat containing 8 family, member A	1.56±0.06
<i>PPP1R14C</i>	Protein phosphatase 1, regulatory (inhibitor) subunit 14C	1.70±0.10
<i>ABCC2</i>	ATP-binding cassette, sub-family C (CFTR/MRP), member 2	2.11±0.78
B, Apoptosis (upregulation)		
Gene symbol	Gene name	Fold change
<i>IRF7</i>	Interferon regulatory factor 7	2.97±0.64
<i>TNFSF10</i>	Tumor necrosis factor (ligand) superfamily, member 10	2.40±0.88
<i>PMAIP1</i>	Phorbol-12-myristate-13-acetate-induced protein 1	2.28±0.20
<i>BCL2L11</i>	Bcl2-like 11 (apoptosis facilitator)	2.24±0.28
<i>APAF1</i>	Apoptotic peptidase activating factor 1	2.15±0.13
<i>BBC3</i>	Bcl2 binding component 3	2.10±0.11
<i>CASP1</i>	Caspase 1, apoptosis-related cysteine peptidase	2.02±0.13
<i>CASP3</i>	Caspase 3, apoptosis-related cysteine peptidase	1.81±0.15
<i>CASP4</i>	Caspase 4, apoptosis-related cysteine peptidase	1.72±0.07
<i>TNFRSF21</i>	Tumor necrosis factor receptor superfamily, member 21	1.68±0.16
<i>HRK</i>	Harakiri, Bcl2interacting protein	1.59±0.08
<i>FAS</i>	Fas cell surface death receptor	1.53±0.04
C, Cell cycle (downregulation)		
Gene symbol	Gene name	Fold change
<i>CDC25C</i>	Cell division cycle 25C	-2.21±0.55
<i>E2F1</i>	E2F transcription factor 1	-1.79±0.27
<i>PKMYT1</i>	Protein kinase, membrane associated tyrosine/threonine 1	-1.76±0.20

Table I. Continued.

C, Cell cycle (downregulation)		
Gene symbol	Gene name	Fold change
<i>RBL1</i>	Retinoblastoma-like 1	-1.75±0.17
<i>ORC5</i>	Origin recognition complex, subunit 5	-1.72±0.02
<i>MCM6</i>	Minichromosome maintenance complex component 6	-1.72±0.10
<i>CCNE2</i>	Cyclin E2	-1.63±0.10
<i>CCNB1</i>	Cyclin B1	-1.58±0.09
<i>PCNA</i>	Proliferating cell nuclear antigen	-1.56±0.05

Data are presented as the mean of fold change ± standard deviation.

'G₁ to S cell cycle control', and 'DNA Replication' (Fig. 2B). Microarray analysis revealed that the expression of 25 genes belonging to the 'Nuclear Receptors Meta-Pathway', such as *CDKN1C* and *PGC-1α* and 12 apoptosis-related genes, such as *CASP3* and *FAS*, were upregulated. A total of nine cell cycle-related genes, including *CDC25C*, *CCNE2* and *CCNB1* were downregulated (Table I). RT-qPCR validated the aforementioned findings (Fig. 3).

Reduction of cell proliferation and induction of TIG113 apoptosis cells by *ERRα* silencing. As silencing of *ERRα* downregulates cell cycle-related genes and upregulates apoptosis-related genes in fibroblasts, cell proliferation and apoptosis analyses were performed. *ERRα* was silenced in TIG113 cells and cell proliferation was evaluated every 24 h. Cells continued to proliferate for up to 72 h in siNC. By contrast, in *ERRα*-silenced TIG113 cells, cell proliferation was significantly reduced after 24 h and the difference in cell proliferation increased after 48 and 72 h, suggesting that cell proliferation was suppressed in *ERRα*-silenced TIG113 (Fig. 4A). Furthermore, in the scratch wound healing assay, the migration percentage of TIG113 cells treated with siNC was 68.9%, whereas it decreased to 32.8% with siERRA (Fig. 4B and C).

As silencing of *ERRα* increased the expression of apoptosis-related genes (Table I and Fig. 3), whether apoptosis was induced was examined. The activity of poly caspase, an apoptosis induction-related enzyme, increased ~2-fold 72 h after transfection with siERRA (Fig. 4D). These results suggest that apoptosis was induced in *ERRα*-silenced TIG113 cells.

Silencing *ERRα* causes cell cycle arrest in TIG113 cells. TIG113 cells were treated with siERRA for 72 h prior to cell cycle analysis. The siERRA treatment significantly increased the proportion of Sub-G₁ phase cells and decreased the proportion of S and G₂/M phase cells (Fig. 5A and B).

Quantification of type I collagen and hyaluronan. ELISA revealed that the amount of type I collagen produced by TIG113 cells was significantly decreased after transfection with siERRA for 72 h (Fig. S2A). Similarly, the amount of hyaluronic acid was significantly decreased after transfection with siERRA (Fig. S2B).

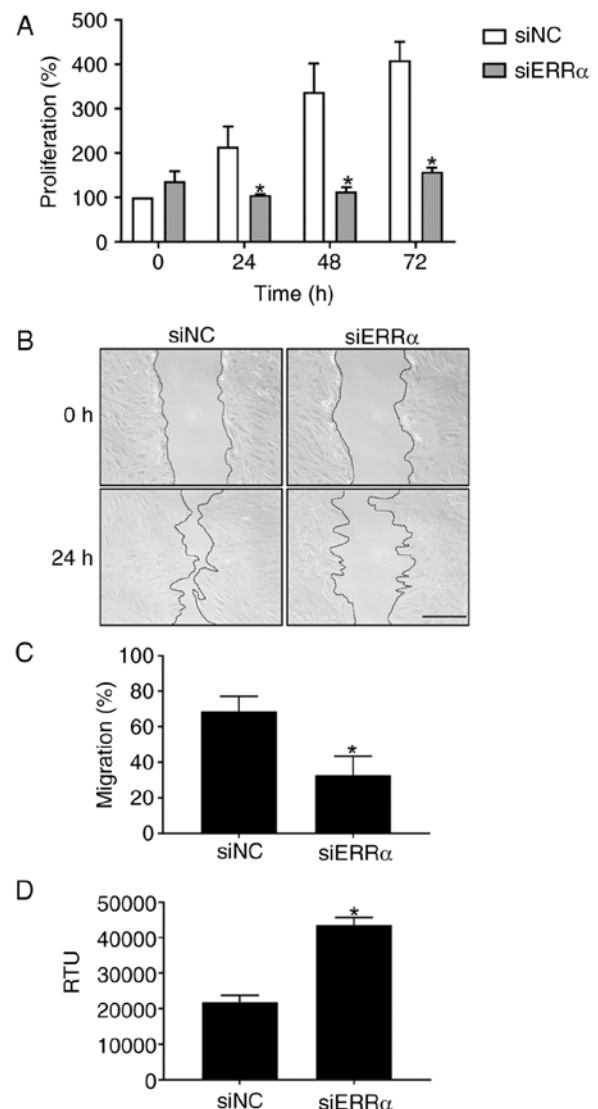


Figure 4. Effect of *ERRα* knockdown on proliferation and apoptosis in TIG113 cells. TIG113 cells were transfected with siERRA or siNC and cultured for 24-72 h. (A) Proliferation of TIG113 cells was determined every 24 h following siERRA transfection. (B) Following transfection of siRNA for 24 h, it was scratch-wounded and cultured for 48 h. Scale bar, 500 μm. (C) Migration area was calculated using the ImageJ software. (D) Apoptosis of TIG113 cells was determined 72 h after siERRA transfection. The data represent the mean ± standard deviation of at least three independent experiments. *P<0.05 vs. siNC. *ERRα*, estrogen-related receptor α; si, small interfering; NC, negative control; RFU, relative fluorescent unit.

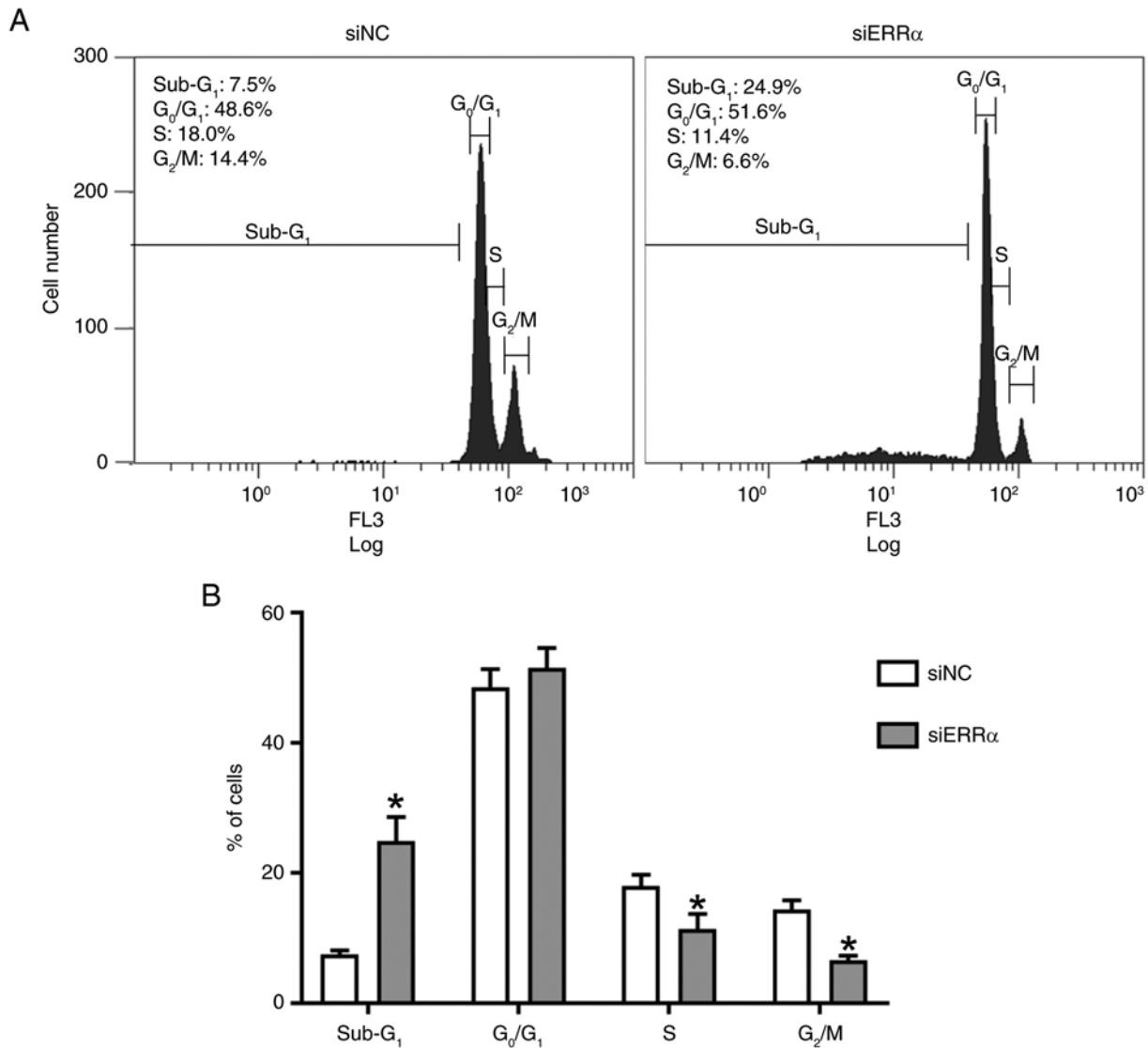


Figure 5. Effect of *ERRα* silencing on the cell cycle in TIG113 cells. Cell cycle analysis in TIG113 cells treated with siERR α or siNC for 72 h prior to DNA staining and fluorescence-activated cell sorting. (A) Cell cycle plots. (B) Percentages of cells in the Sub-G₁, G₀/G₁, S and G₂/M phases. Data were analyzed using the MultiCycle AV software and represent the mean \pm standard deviation of the mean of three independent experiments. * $P < 0.05$ vs. siNC. ERR α , estrogen-related receptor α ; si, small interfering; NC, negative control.

Discussion

ERRα is expressed in skin tissue, but its function is unknown. In the present study, *ERRα* was silenced by siRNA in human skin fibroblasts and its function was analyzed. *ERRα*, *ERRβ* and *ERRγ* are expressed in keratinocytes of the skin epidermis and it has been reported that only *ERRγ* is expressed in fibroblasts (15-17). However, in the present study, the expression levels of *ERRα* in siNC-treated TIG113 cells in microarrays was higher than that of *ERRβ* and γ . As the present study mainly aimed to clarify the function of *ERRα* in TIG113 cells, the comparison of the expression of *ERRα*, β and γ , as well as the estrogen receptor, was only a supplementary analysis and thus absolute quantitative expression analysis was not performed. However, detailed analysis using absolute quantification is required to compare the expression levels of ERRs and estrogen receptors α and β in the future. Furthermore, because only a few studies reported expression of ERRs in skin tissues and cells, further analysis with more specimens is required.

Silencing of *ERRα* decreased the expression of cell cycle-related genes such as *CDC25C*, *CCNE2* and *CCNB1*. *CDC25C* is known to control the transition from the G₁ phase to the S phase and the transition from the G₂ phase to the M phase (29). In addition, cyclin E binds to cyclin-dependent kinase 2 in the G₁ phase to form a complex that is required for the cell cycle transition from the G₁ phase to the S phase where DNA replication is initiated (30) and *CCNB1* is a regulatory protein involved in mitosis (31). Furthermore, silencing of *ERRα* increases the expression of *CDKN1C*, a known cell cycle inhibitor (32). Expression of these genes related to the cell cycle was decreased and cell proliferation was suppressed in *ERRα*-silenced TIG113, suggesting that a normal cell cycle did not occur. Cell cycle analysis showed that siERR α knock-down decreased the number of cells in the S and G₂/M phases. *ERRα* regulates *CDC25C* and *CCNB1* in gastric cancer cells, suggesting that it also regulates these genes in fibroblasts (33).

Silencing of *ERRα* enhanced apoptosis and the expression of apoptosis induction-related genes such as *CASP3*

and *FAS*. Furthermore, Sub-G₁ phase cells were increased in siERR α -treated TIG113 cells. An increase in the Sub-G₁ phase was observed in apoptotic cells (34), suggesting that apoptosis was induced by siERR treatment. Caspases are a family of proteases that play central roles in numerous processes, including cell death and inflammation and *CASP3* is an important mediator of apoptosis (35). *FAS* is a type I transmembrane protein and apoptosis is induced upon binding of the Fas ligand (36,37). The results of the present study suggested that increased expression of these apoptosis-related genes induce cell death in ERR α -silenced TIG113 cells. The *p53* gene encodes a protein that has the function of regulating suppression of the cell growth cycle such as DNA repair, cell growth arrest and apoptosis (38). It has recently been reported that ERR α and p53 protein directly bind to regulate colon cancer growth through regulation of mitochondrial biogenesis and that knockdown of ERR α suppresses *p53* gene expression and impairs mitochondrial biogenesis (39). Although no change was observed in the expression level of *p53* in this study (data not shown), it is possible that silencing of *ERR α* abolished its interaction with p53 and reduced mitochondrial biogenesis. ERR α contributes to the proliferation of some cancer cells and knockdown of ERR α reduces cell proliferation and induces apoptosis (40-42), consistent with the results of the present study. This suggested that ERR α also contributes to cell proliferation in normal skin fibroblasts.

The PGC-1 family includes PGC-1 α , PGC-1 β and PGC-1-related coactivators, which regulate mitochondrial biogenesis (43). PGC-1 α induces ERR α expression and interacts with ERR α (44) and the ERR α /PGC-1 α axis is known to decrease with aging, accelerating osteoporosis, kidney dysfunction, sarcopenia and neurodegeneration (7). Furthermore, the expression of PGC-1 α is enhanced in the myocardium of ERR α -null mice (45), consistent with the findings of the present study. Although the mechanism is not clear, it is possible that the silencing of ERR α in fibroblasts compensates for the enhancement of PGC-1 α expression, or that ERR α regulates the expression of PGC-1 α .

Thus, knocking down ERR α altered various genes, leading to cell cycle modifications and the induction of apoptosis. However, the present study was unable to identify any genes directly regulated by ERR α . Future research should focus on identifying the direct targets of ERR α .

In the skin, fibroblasts secrete components that contribute to skin antiaging, such as type I collagen and hyaluronan. It was hypothesized that the decrease in cell proliferation was due to a decrease in these components. Furthermore, when TIG113 cells were treated with siERR α , the amount of type I collagen and hyaluronan secreted into the culture supernatant decreased. These results suggested that ERR α may also be an important factor for skin antiaging.

ERR α is an orphan nuclear receptor that can be activated by exogenous agonists such as phytoestrogens such as genistein and daidzein (46), which exhibit estrogenic activity and are found in plants. These compounds share target genes with estrogen receptors and phytoestrogens may activate the ERR pathway, potentially contributing to skin fibroblast proliferation. As estrogen is not an ERR ligand and does not activate ERR, the present study did not investigate the activation of ERR α by estrogen treatment. However, given that various phytoestrogens

may act as ligands for ERR α , future research should explore these possibilities to uncover new activators of ERR α .

ERR is expressed in skin tissue, but its function is unknown. The present study found that suppression of ERR α expression using siRNA suppresses cell proliferation and induces apoptosis. As a reduction in skin fibroblasts accelerates skin aging, the discovery of new exogenous ligands for ERR α and activation of ERR α may lead to the development of new skin antiaging treatments.

Acknowledgements

Not applicable.

Funding

The present study was partly supported by the Japan Society for the Promotion of Science KAKENHI (grant nos. 20K02402 and 23K02038).

Availability of data and materials

The data generated in the present study may be requested from the corresponding author. The TIG113 microarray datasets generated in the present study may be found in the Gene Expression Omnibus under accession number GSE245234 or at the following URL: <https://www.ncbi.nlm.nih.gov/geo/query/acc.cgi?acc=GSE245234>.

Authors' contributions

NN designed the study. NN, TN, MN, CH and KH performed the experiments and analyzed the data. NN, MN and KH confirm the authenticity of all the raw data. NN and CH wrote the original manuscript. All authors read and approved the final version of the manuscript.

Ethics approval and consent to participate

Not applicable.

Patient consent for publication

Not applicable.

Competing interests

The authors declare that they have no competing interests.

References

1. Giguère V, Yang N, Segui P and Evans RM: Identification of a new class of steroid hormone receptors. *Nature* 331: 91-94, 1988.
2. Horard B and Vanacker JM: Estrogen receptor-related receptors: Orphan receptors desperately seeking a ligand. *J Mol Endocrinol* 31: 349-357, 2003.
3. Huss JM, Imahashi K, Dufour CR, Weinheimer CJ, Courtois M, Kovacs A, Giguère V, Murphy E and Kelly DP: The nuclear receptor ERR α is required for the bioenergetic and functional adaptation to cardiac pressure overload. *Cell Metab* 6: 25-37, 2007.
4. Deblois G and Giguère V: Functional and physiological genomics of estrogen-related receptors (ERRs) in health and disease. *Biochim Biophys Acta* 1812: 1032-1040, 2011.

5. Fan W, He N, Lin CS, Wei Z, Hah N, Waizenegger W, He MX, Liddle C, Yu RT, Atkins AR, *et al*: *ERRγ* promotes angiogenesis, mitochondrial biogenesis, and oxidative remodeling in PGC1 α/β -deficient muscle. *Cell Rep* 22: 2521-2529, 2018.
6. Schreiber SN, Emter R, Hock MB, Knutti D, Cardenas J, Podvinec M, Oakeley EJ and Kralli A: The estrogen-related receptor alpha (*ERRalpha*) functions in PPARgamma coactivator 1alpha (PGC-1alpha)-induced mitochondrial biogenesis. *Proc Natl Acad Sci USA* 101: 6472-6477, 2004.
7. Vernier M and Giguère V: Aging, senescence and mitochondria: The PGC-1/*ERR* axis. *J Mol Endocrinol* 66: R1-R14, 2021.
8. Luo J, Sladek R, Bader JA, Matthyssen A, Rossant J and Giguère V: Placental abnormalities in mouse embryos lacking the orphan nuclear receptor *ERR-beta*. *Nature* 388: 778-782, 1997.
9. Giguère V: To *ERR* in the estrogen pathway. *Trends Endocrinol Metab* 13: 220-225, 2002.
10. Brincat MP, Baron YM and Galea R: Estrogens and the skin. *Climacteric* 8: 110-123, 2005.
11. Stern R and Maibach HI: Hyaluronan in skin: Aspects of aging and its pharmacologic modulation. *Clin Dermatol* 26: 106-122, 2008.
12. Thornton MJ: Estrogens and aging skin. *Dermatoendocrinol* 5: 264-270, 2013.
13. Haczynski J, Tarkowski R, Jarzabek K, Slomczynska M, Wolczynski S, Magoffin DA, Jakowicki JA and Jakimiuk AK: Human cultured skin fibroblasts express estrogen receptor alpha and beta. *Int J Mol Med* 10: 149-153, 2002.
14. Saito K and Cui H: Emerging roles of estrogen-related receptors in the brain: Potential interactions with estrogen signaling. *Int J Mol Sci* 19: 1091, 2018.
15. Bertil E, Bolzinger MA, André V, Rousselle P and Damour O: Expression of oestrogen-related receptor alpha in human epidermis. *Exp Dermatol* 17: 208-213, 2008.
16. Krahn-Bertil E, Dos Santos M, Damour O, Andre V and Bolzinger MA: Expression of estrogen-related receptor beta (*ERRbeta*) in human skin. *Eur J Dermatol* 20: 719-723, 2010.
17. Krahn-Bertil E, Bolzinger MA, Andre V, Orly I, Kanitakis J, Rousselle P and Damour O: Expression of estrogen-related receptor gamma (*ERRgamma*) in human skin. *Eur J Dermatol* 18: 427-432, 2008.
18. Liu D, Zhang Z, Gladwell W and Teng CT: Estrogen stimulates estrogen-related receptor alpha gene expression through conserved hormone response elements. *Endocrinology* 144: 4894-4904, 2003.
19. Fujimoto J, Nakagawa Y, Toyoki H, Sakaguchi H, Sato E and Tamaya T: Estrogen-related receptor expression in placenta throughout gestation. *J Steroid Biochem Mol Biol* 94: 67-69, 2005.
20. Hoffmann MJ, Florl AR, Seifert HH and Schulz WA: Multiple mechanisms downregulate CDKN1C in human bladder cancer. *Int J Cancer* 114: 406-413, 2005.
21. Thamizhanambi TP, Rameshkumar A, Ramya R, Krishnan R, Dineshkumar T and Nandhini G: Analysis of metabolic regulators PGC1- α and PGC1- β in oral squamous cell carcinoma with and without hyperglycemia. *Asian Pac J Cancer Prev* 23: 2797-2803, 2022.
22. Jafari N, Zargar SJ, Yassa N and Delnavazi MR: Induction of apoptosis and cell cycle arrest by *Dorema glabrum* root extracts in a gastric adenocarcinoma (AGS) cell line. *Asian Pac J Cancer Prev* 17: 5189-5193, 2016.
23. Piri-Gharaghie T, Ghajari G, Hassanpoor M, Jegargoshe-Shirin N, Soosanirad M, Khayati S, Farhadi-Biregani A and Mirzaei A: Investigation of antibacterial and anticancer effects of novel nisomal formulated Persian Gulf Sea cucumber extracts. *Heliyon* 9: e14149, 2023.
24. Zhang W, Shang X, Yang F, Han W, Xia H, Lu N, Liu Y and Wang X: CDC25C as a predictive biomarker for immune checkpoint inhibitors in patients with lung adenocarcinoma. *Front Oncol* 12: 867788, 2022.
25. Chen M, Wu R, Li G, Liu C, Tan L, Xiao K, Ye Y and Qin Z: Motor neuron and pancreas homeobox 1/*HLXB9* promotes sustained proliferation in bladder cancer by upregulating *CCNE1/2*. *J Exp Clin Cancer Res* 37: 154, 2018.
26. Du Y, Zheng Y, Yu K, Zhan C and Qiao T: Genome-wide analyses of lung cancer after single high-dose radiation at five time points (2, 6, 12, 24, and 48 h). *Front Genet* 14: 1126236, 2023.
27. Livak KJ and Schmittgen TD: Analysis of relative gene expression data using real-time quantitative PCR and the 2(-Delta Delta C(T)) method. *Methods* 25: 402-408, 2001.
28. Nanashima N, Horie K, Chiba M, Nakano M, Maeda H and Nakamura T: Anthocyanin-rich blackcurrant extract inhibits proliferation of the MCF10A healthy human breast epithelial cell line through induction of G0/G1 arrest and apoptosis. *Mol Med Rep* 16: 6134-6141, 2017.
29. Perdiguero E and Nebreda AR: Regulation of Cdc25C activity during the meiotic G2/M transition. *Cell Cycle* 3: 733-737, 2004.
30. Fagundes R and Teixeira LK: Cyclin E/*CDK2*: DNA replication, replication stress and genomic instability. *Front Cell Dev Biol* 9: 774845, 2021.
31. Hayward D, Alfonso-Pérez T and Gruneberg U: Orchestration of the spindle assembly checkpoint by *CDK1-cyclin B1*. *FEBS Lett* 593: 2889-2907, 2019.
32. Matsuoka S, Edwards MC, Bai C, Parker S, Zhang P, Baldini A, Harper JW and Elledge SJ: p57^{KIP2}, a structurally distinct member of the p21^{CIP1} Cdk inhibitor family, is a candidate tumor suppressor gene. *Genes Dev* 9: 650-662, 1995.
33. Li FN, Zhang QY, Li O, Liu SL, Yang ZY, Pan LJ, Zhao C, Gong W, Shu YJ and Dong P: *ESRRA* promotes gastric cancer development by regulating the *CDC25C/CDK1/CyclinB1* pathway via *DSN1*. *Int J Biol Sci* 17: 1909-1924, 2021.
34. Bedner E, Li X, Gorczyca W, Melamed MR and Darzynkiewicz Z: Analysis of apoptosis by laser scanning cytometry. *Cytometry* 35: 181-195, 1999.
35. Orlinick JR and Chao MV: TNF-related ligands and their receptors. *Cell Signal* 10: 543-551, 1998.
36. Nagata S and Golstein P: The Fas death factor. *Science* 267: 1449-1456, 1995.
37. Akagi T, Yoshino T and Kondo E: The Fas antigen and Fas-mediated apoptosis in B-cell differentiation. *Leuk Lymphoma* 28: 483-489, 1998.
38. Götz C and Montenarh M: p53: DNA damage, DNA repair, and apoptosis. *Rev Physiol Biochem Pharmacol* 127: 65-95, 1996.
39. De Vitto H, Ryu J, Calderon-Aparicio A, Monts J, Dey R, Chakraborty A, Lee MH, Bode AM and Dong Z: Estrogen-related receptor alpha directly binds to p53 and cooperatively controls colon cancer growth through the regulation of mitochondrial biogenesis and function. *Cancer Metab* 8: 28, 2020.
40. Matsushima H, Mori T, Ito F, Yamamoto T, Akiyama M, Kokabu T, Yoriki K, Umemura S, Akashi K and Kitawaki J: Anti-tumor effect of estrogen-related receptor alpha knockdown on uterine endometrial cancer. *Oncotarget* 7: 34131-34148, 2016.
41. Sun P, Mao X, Gao M, Huang MM, Chen LL, Ruan GY, Huang WY, Braicu EI and Schouli J: Novel endocrine therapeutic strategy in endometrial carcinoma targeting estrogen-related receptor α by *XCT790* and *siRNA*. *Cancer Manag Res* 10: 2521-2535, 2018.
42. Zhang J, Guan X, Liang N and Li S: Estrogen-related receptor alpha triggers the proliferation and migration of human non-small cell lung cancer via interleukin-6. *Cell Biochem Funct* 36: 255-262, 2018.
43. Scarpulla RC: Metabolic control of mitochondrial biogenesis through the PGC-1 family regulatory network. *Biochim Biophys Acta* 1813: 1269-1278, 2011.
44. Schreiber SN, Knutti D, Brogli K, Uhlmann T and Kralli A: The transcriptional coactivator PGC-1 regulates the expression and activity of the orphan nuclear receptor estrogen-related receptor alpha (*ERRalpha*). *J Biol Chem* 278: 9013-9018, 2003.
45. Dufour CR, Wilson BJ, Huss JM, Kelly DP, Alaynick WA, Downes M, Evans RM, Blanchette M and Giguère V: Genome-wide orchestration of cardiac functions by the orphan nuclear receptors *ERRalpha* and *gamma*. *Cell Metab* 5: 345-356, 2007.
46. Suetsugu M, Su L, Karlsberg K, Yuan YC and Chen S: Flavone and isoflavone phytoestrogens are agonists of estrogen-related receptors. *Mol Cancer Res* 1: 981-991, 2003.



Copyright © 2024 Nanashima et al. This work is licensed under a Creative Commons Attribution-NonCommercial-NoDerivatives 4.0 International (CC BY-NC-ND 4.0) License.